Probabilistic simulation of advection-reaction-dispersion equation using random lattice Boltzmann method

Ali Akbar Hekmatzadeh [a, 1], Ali Adel [a], Farshad Zarei [a], Ali Torabi Haghighi [b]

a- Department of Civil and Environmental Engineering, Shiraz University of Technology, Po. Box 71555-313, Shiraz, Iran, email: hekmatzadeh@sutech.ac.ir

b- Water Resources and Environmental Engineering Research Group, University of Oulu, PO Box 4300, FIN-90014, Finland, email: Ali.TorabiHaghighi@oulu.fi

Abstract

Mass transfer is subject to numerous sources of uncertainties due to scarcity of observational data. In this research, a numerical procedure was developed for the probabilistic study of a two-dimensional advection-dispersion problem, while considering chemical reactions. Innovatively, the lattice Boltzmann method was coupled with the concept of random field theory for the probabilistic simulations. The effects of various coefficients of variations (COV) and a number of autocorrelation distances were considered for the stochastic parameters, including dispersion coefficient, pore velocity, and the reaction term. The results indicated that the introduced probabilistic framework can be employed to effectively describe the effects of uncertainties in parameters related to the advection-dispersion equation. Moreover, it was deduced that the mass travel time and the time-concentration curves were influenced significantly by the variations of COV and autocorrelation distance for pore velocity. Interestingly, the mass transfer in the transverse direction increased (through the dispersion phenomenon) with a rise in the values of COV for longitudinal pore velocity. However, different values of COV and autocorrelation distances for the dispersion coefficient and the reaction term caused small alterations in the mass travel time and time-concentration curve.

Keywords: Lattice Boltzmann method, Advection-reaction-dispersion equation, Random field, Mass travel time, Time-concentration curve.

[1] Corresponding author. Tel.: +98 71 37277656, Mobile: +98 9177140175, Fax: +98 71 37277656. Email address: hekmatzadeh@sutech.ac.ir & hekmatzadeh@yahoo.com (A. A. Hekmatzadeh).

Nomenclature

C	Mass concentration	ACM	Auto-correlation matrix
D	Dispersion coefficient	n_e	Number of random field elements
U	Pore velocity	L	Lower triangular matrix
λ	Reaction rate	G_i	Standard Gaussian random field
c	Lattice velocity	Z_j	An indicator of standard normal distribution
τ	Single relaxation time	RV	Random variable
f_i	Particle distribution function	COV	Coefficient of variations
f_i^{eq}	Equilibrium distribution function	μ_{RV}	Mean of random variable
c_i	Lattice velocity in direction i	σ_{RV}	Standard deviation of random variable
w_i	Weight coefficient in the lattice direction i	$\mu_{\ln RV}$	Mean of logarithmic random variable
Pe^*	Scaled Peclet number	$\sigma_{\ln RV}$	Standard deviation of logarithmic random variable
Cr	Courant number	$\rho(RV_1, RV_2)$	Cross-correlation coefficient between RV_1 and RV_2
Pe_G	Grid Peclet number	G_{i-RV_j}	Modified standard Gaussian random field for RVj
c_s	Constant parameter for the lattice scheme	ACF	Auto-correlation function
L_x	Horizontal autocorrelation distance	Y_1	Transversal locations of input pollution plume
L_y	Vertical autocorrelation distance	Y_2	Transversal locations of input pollution plume
$\rho(\tau_{x_{ij}}, \tau_{y_{ij}})$	Auto-correlation coefficient	W	Domain width
$\tau_{x_{ij}}$	Horizontal distance between the centroid of the ith and jth elements	$T_{c=5}$	Mass travel time (concentration is 5 mg/lit)
$\tau_{y_{ij}}$	Vertical distance between the centroid of the ith and jth elements	$T_{c=20}$	Mass travel time (concentration is 20 mg/lit)

1. Introduction

The advection-dispersion equation, also called convection-diffusion equation, governs several natural phenomena, including mass, energy, turbulence, and heat transfer [1]. The incomplete knowledge of information and various assumptions in the mathematical modeling end up with uncertainty in the model constants such as dispersion coefficient and velocity [2]. In addition, in cases such as pollution transport in groundwater resources, natural soil is faced with heterogeneity as a result of geological formations, leading to higher variability of physical properties [3, 4]. Mass transfer modeling is essential for management or remediation of groundwater resources all over

the world [4, 5]. To deal with the above-mentioned uncertainties, stochastic methods are combined with the mathematical or numerical solutions of advection-dispersion equation [2, 6].

A host of studies have made use of the random field theory to describe the uncertainty in different fields of engineering, including geotechnical, structural, and water engineering. Griffiths et al. [7] and Lo and Leung [8] employed random the field theory coupled with the finite element method to investigate the probability of failure of an embankment slope. Regarding the seepage phenomenon, several types of stochastic analyses have been conducted by Cho [9], Tan et al. [10], Hekmatzadeh et al. [11], Srivastava et al. [12], Ahmed [13, 14], and Griffiths and Fenton [15-18] to estimate the probability distribution of exit gradient beneath a dam. Do et al. [19] applied random field concept for the Young's modulus in the analysis of structures.

In terms of mass transfer, as with pollution transport, a few studies have been conducted to examine the effect of spatial variability. The effect of random soil hydraulic conductivity on solute transport was analyzed using Monte Carlo simulation (MCS) by Wang and Huang [20]. In the aforementioned study, the random permeability field was generated using successive random addition. Then, groundwater flow and solute transport were simulated using well-known finite difference MODFLOW code and MT3DMS code, respectively. In addition, the first order reliability method (FORM) has been combined with a finite element code to develop a stochastic scheme for modeling the groundwater pollution [21]. Shi et al. [2] used stochastic collection method to consider the influence of a heterogeneous aquifer on the advection dispersion equation. The uncertainty in the advection and dispersion terms of a solute transport problem was studied by Li et al. [5] using stochastic finite element method.

In the majority of aforementioned stochastic studies which employed the random field concept, thousands of random field realizations have been produced, and then for each realization, the governing differential equation such as Laplace equation has been solved using finite element methods or finite difference methods [19, 22, 23]. Regarding mass transfer problems that are generally time-dependent, the abovementioned procedure may not be efficient when it comes to computational time. Moreover, numerical solutions of time-dependent problems may suffer from instability issues when the time step is not small enough [24, 25]. In addition, advection-dominated mass transfer problem may face artificial numerical oscillations when the grid size is large. One solution to eliminate theses over/undershoots and guarantee the stability is to reduce the grid size

[24, 26, 27]. However, the smaller the time step and grid size are, the more computational time is required, which is challenging in the random field problems.

In the last decade, the lattice Boltzmann (LB) method has emerged as a robust numerical tool to solve time-dependent problems, including advection-dispersion equations [28-30]. Not only are the LB methods efficient and fast computational methods, but also their stability is admirable, especially in advection-dominated mass transport problems [26, 31]. Easy programing in addition to modeling complex boundary conditions are other advantages of the LB method [26, 30]. In addition, the LB method shows superior capability to comply with parallel programming techniques utilizing graphics processing unit (GPU) [32]. The central idea of the LB method is to provide a bridge between microscopic distribution function and macroscopic variables such as mass concentration [33]. Different lattice configurations have been introduced to solve advection-dispersion equation, comprising D2Q4, D2Q5 in addition to D2Q9 for two-dimensional problems [31, 33].

To the author's best knowledge, no study was found to combine random field discretization with the LB method in order to investigate stochastically an engineering problem [10, 13, 23, 34, 35]. Regarding the advection-dispersion equation, few studies make use of the stochastic field to investigate mass transfer, especially in a transient state [6, 36-38]. Besides, it is beneficial to determine the effects of stochastic reaction term in the advection-dispersion equation coupled with the chemical reaction of mass.

The main motivation of this study is to carry out probabilistic analysis of mass transfer using random field theory in two dimensions. For this purpose, the LB method is combined with random field discretization for the first time. Among several schemes of the LB method, D2Q5 Scheme with single relaxation time was chosen due to its high level of accuracy and high computational speed [26, 32]. The Cholesky decomposition method together with MCS and exponential autocorrelation function were used to generate random parameters, including dispersion coefficient, pore velocity, and chemical reaction term. Moreover, lognormal distribution was assumed for the parameters mentioned above. The mass travel time and the time-concentration curve were considered as objective parameters for stochastic investigations. The influences of different autocorrelation distances in addition to several coefficients of variations (COV) are

surveyed comprehensively. Finally, the effects of cross-correlation between the realizations of dispersion coefficient and the realizations of pore velocity were taken into consideration.

2. Mass transfer

Mass transfer in a system such as porous media is modeled mathematically using the mass balance relationship. Assuming linear chemical reaction between the mass and the system, the governing equation of the mass transfer in 2D is written as Eq. (1), which is called advection-reaction-dispersion equation [24].

$$\frac{\partial C}{\partial t} = D\ \frac{\partial^2 C}{\partial x^2} + D\ \frac{\partial^2 C}{\partial y^2} - U\frac{\partial C}{\partial x} - \lambda C \qquad (1)$$

where C is the mass concentration, D represents the dispersion coefficients along both x and y directions, U indicates the pore velocity along x direction, and λ is the chemical reaction rate of mass with the media. It should be noted that Eq. (1) describes the mass transfer phenomenon in isotropic circumstances, and consequently, the dispersion coefficients along x and y directions are identical.

3. Review of lattice Boltzmann method

The mathematical model of several natural phenomena can be described using LB equation [31, 33]. The discrete form of LB equation with regard to the Bhatnagar, Gross and Krook (BGK) collision operator is expressed as [33]:

$$f_i\left(x + c_i\Delta t, t + \Delta t\right) = f_i\left(x,t\right) + \frac{\Delta t}{\tau}\left[f_i^{eq}\left(x,t\right) - f_i\left(x,t\right)\right] \qquad (2)$$

where τ is the single relaxation time (SRT), f_i signifies the particle distribution function along the lattice direction i, f_i^{eq} represents the equilibrium distribution function (EDF) of particles, and c_i stands for the lattice velocity in direction i, which is defined by Eq. (3).

$$c_i = \begin{cases} (0,0) & i = 0 \\ \left(\cos\left[(i-1)\pi/2\right], \sin\left[(i-1)\pi/2\right]\right)c & i = 1,\ 2\ ,\ 3,\ 4 \end{cases} \qquad (3)$$

In this relation, c is the lattice velocity ($c = \Delta x / \Delta t$). Regarding advection-dispersion equation, the relaxation time and the equilibrium distribution function of the LB equation are stated as follows [27]

$$\tau_{ad} = \frac{D}{\Delta t c_s^2} + \frac{1}{2} \tag{4}$$

$$f_i^{eq} = w_i C\left[1 + \frac{\vec{U}.c_i}{c_s^2}\right] \tag{5}$$

where $c_s = c/\sqrt{3}$ for D2Q5 scheme. w_i is the weight coefficient in the lattice direction i, defined by relations (6) for D2Q5 scheme [39]:

$$\begin{cases} w_i = \frac{2}{6} & i = 0 \\ w_i = \frac{1}{6} & i = 1,\ 2,\ 3,\ 4 \end{cases} \tag{6}$$

The mass concentration is estimated by the summation of particle distribution function alongside all lattice directions [29, 33]:

$$C = \sum_i f_i(x,t) \tag{7}$$

Considering the Dirichlet boundary condition where the variable is specified at the left border, the particle distribution function in direction 1 (see Fig. 1) is computed using Eq. (8) [40]:

$$f_1 = C - f_0 - f_2 - f_3 - f_4 \tag{8}$$

where f_0, f_2, f_3, f_4 are obtained from the streaming process. In terms of the Neumann boundary condition, where the variable gradient is identified at the eastern border of the domain, f_1 is estimated using Eq. (9) [40].

$$f_{1(n-1)} = \sum f_{i(n)} - f_{0(n-1)} - f_{2(n-1)} - f_{3(n-1)} - f_{4(n-1)} \tag{9}$$

4. Random field theory

The constants of advection-reaction-dispersion equation, including the dispersion coefficient, the pore velocity, and the reaction term, may be faced with spatial variability. In case of pollution

transport in the groundwater, the properties of natural soil such as dispersion coefficient encounter special variability due to the geological soil formations [3, 41]. The spatial variability can be modeled using random field theory by the employment of a suitable probability density function (PDF) and an auto-correlation function (ACF) [16]. In the random field approach, values of soil properties are assumed as random variables in different locations. Considering MCS, random numbers are generated for soil parameters at these locations in association with their PDF. Afterwards, thousands of analyses predicated on the generated random fields were performed. Generally, analyses were performed with a mesh identical to that used for deterministic analysis. Accordingly, the variables of interest (such as mass travel time) are obtained from every realization, forming the probability distribution for the quantities under study [11, 42].

Concerning the lognormal distribution for the parameters mentioned above, the mean and standard deviation ($\mu_{\ln RV}$ and $\sigma_{\ln RV}$) of the random variables (RV) are estimated using Eqs. (10) and (11), respectively [12, 16].

$$\mu_{\ln RV} = \ln\left(\mu_{RV}\right) - \frac{1}{2}\sigma^2_{\ln RV} \tag{10}$$

$$\sigma_{\ln RV} = \sqrt{\ln\left(1 + \frac{\sigma^2_{RV}}{\mu^2_{RV}}\right)} = \sqrt{\ln\left(1 + COV^2_{RV}\right)} \tag{11}$$

where μ_{RV} and σ_{RV} are the mean and standard deviation of random variable. One advantage of the lognormal distribution is that there is no possibility for the negative values [43].

There are a number of ACF to describe the degree of correlation between two points irrespective of their global coordinates [41, 44]. The most applied ACF used to illustrate the spatial variability of soil characteristics is the exponential auto-correlation function [22, 45], which is given by:

$$\rho\left(\tau_{x_{ij}}, \tau_{y_{ij}}\right) = \exp\left(-\frac{\tau_{x_{ij}}}{L_x} - \frac{\tau_{y_{ij}}}{L_y}\right) = \exp\left(-\frac{\left|x_i - x_j\right|}{L_x} - \frac{\left|y_i - y_j\right|}{L_y}\right) \tag{12}$$

here, $\tau_{X_{ij}} = \left|x_i - x_j\right|$ and $\tau_{y_{ij}} = \left|y_i - y_j\right|$ are the absolute distances between two points in the horizontal and vertical directions, respectively. L_x and L_y represent the horizontal and vertical autocorrelation distances of stochastic parameter, respectively.

Considering the numerical mesh, the following auto-correlation matrix (ACM) is constructed for the whole domain:

$$ACM = \begin{bmatrix} 1 & \rho\left(\tau_{x_{12}}, \tau_{y_{12}}\right) & \cdots & \rho\left(\tau_{x_{1n_e}}, \tau_{y_{1n_e}}\right) \\ \rho\left(\tau_{x_{21}}, \tau_{y_{21}}\right) & 1 & \cdots & \rho\left(\tau_{x_{2n_e}}, \tau_{y_{2n_e}}\right) \\ \vdots & \vdots & \ddots & \vdots \\ \rho\left(\tau_{x_{n_e1}}, \tau_{y_{n_e1}}\right) & \rho\left(\tau_{x_{n_e2}}, \tau_{y_{n_e2}}\right) & \cdots & 1 \end{bmatrix} \quad (13)$$

where $\rho\left(\tau_{x_{ij}}, \tau_{y_{ij}}\right)$ indicates the autocorrelation coefficient between the centroids of elements. $\tau_{x_{ij}}$ and $\tau_{y_{ij}}$ indicate the distances between the centroid of the ith and the jth elements. In this study, the Cholesky decomposition method [12, 44, 46] was used to generate random values of stochastic parameter. Accordingly, the above-mentioned matrix is decomposed into the product of a lower triangular matrix, L, and its transpose (Eq. (14)).

$$LL^T = ACM \quad (14)$$

Regarding matrix L, the standard Gaussian random field (G_i) can be attained using Eq. (15):

$$G_i = \sum_{j=1}^{i} L_{ij} Z_j \quad , \quad i = 1,2,3, \ldots ,n \quad (15)$$

In the above equation, Z_j follows the standard normal distribution ($\mu = 0$ and $\sigma = 1$). Finally, the values of random variable along x and y directions for each element are estimated as follows:

$$RV_i = \exp\left\{\mu_{\ln RV} + \sigma_{\ln RV} G_i\right\} \quad (16)$$

In a case where two random variables (RV1 and RV2) are correlated with a cross-correlation coefficient ($\rho_{RV1,RV2}$), the parameter G_i in Eq. (16) is replaced with G_{i-RV1} and G_{i-RV2} according to the following relations:

$$\begin{Bmatrix} G_{i-RV1} \\ G_{i-RV2} \end{Bmatrix} = A \begin{Bmatrix} G_{i-RV1-Eq.\ (15)} \\ G_{i-RV2-Eq.\ (15)} \end{Bmatrix} \quad (17)$$

$$AA^T = \begin{bmatrix} 1 & \rho_{RV_1,RV_2} \\ \rho_{RV_1,RV_2} & 1 \end{bmatrix} \quad (18)$$

where G_{i-RV1} and G_{i-RV1} represent the modified standard Gaussian random field for RV_1 and RV_2, respectively, and $G_{i-RV1-Eq.\ (15)}$ and $G_{i-RV2-Eq.\ (15)}$ are computed using Eq. (15) [12, 44, 46]. In the random field generation process of this study, it is assumed that the logarithms of variables are Normally distributed. Here, the cross-correlation coefficient may be assumed between RV_1 and RV_2 or it may be defined between the logarithms of variables. Considering the former case, a correction factor (F), defined below, is multiplied by ρ_{RV_1,RV_2} [47]:

$$F = \frac{\ln(1+\rho_{RV1,RV2}\,COV_i\,COV_j)}{\rho_{RV1,RV2}\sqrt{\ln(1+COV_i^2)\ln(1+COV_j^2)}} \tag{19}$$

The above equation is valid when COV varies between 0.1 to 0.5.

Of note, an identical regular mesh was used for both LB method and the generation of random field (construction of ACM). The LB equation (Eq. (2)) is solved at the mesh points, and it needs mass transfer parameters (D, U, and λ) at every point. However, by the formation of the ACM, these parameters are determined for the element area. Therefore, the properties at every location were set to the average values of adjacent elements [48].

5. Stability

The LB method is an explicit scheme, which may be subject to stability criterion. Hence, time step and spatial resolution should be carefully selected to prevent numerical instability in the solution. Servan-Camas and Tasi [29, 31] specified the stable domain for the LB solution of advection-dispersion equation using von Neumann analysis. Accordingly, the stability domain depends on the scaled Peclet number $Pe^* = (u\,\Delta x / D)(\tau - 0.5)$, the Courant number $Cr = u\,\Delta t / \Delta x$, and the relaxation time, as shown in Fig 1. Regarding the artificial oscillations induced by advection-dominated mass transfer [24], D2Q5 faces numerical over/undershoots when the grid Peclet number $Pe_G = (u\,\Delta x / D)$ is greater than 20 [26]. Hence, mesh resolution should fulfill this criterion.

6. Application to mass transfer problems

6.1. Problem 1

Herein, a two-dimensional solute transport problem is considered in a domain size of $50\ \mathrm{m} \times 50\ \mathrm{m}$. The solute plume with the concentration of 200 mg/lit enters the domain across 10 meters of the left side (Fig. 2a). The initial solute concentration inside the domain is assumed to be zero. The groundwater flow is considered along x direction, while the dispersion happens along both x and y directions. Therefore, the mass can exit the domain through all borders except line MN in Fig 2a.

The advection-reaction-dispersion equation mentioned above (Eq. (1)) contains three stochastic parameters as follows: pore velocity (U), dispersion coefficient (D), and reaction term (λ). These parameters were described using lognormal distribution according to Table 1. It should be noted that lognormal distribution has been widely used by researchers to describe soil stochastic parameters [12, 44, 46]. Different values of autocorrelation distance and coefficient of variations were taken into account for each stochastic parameter (Table 1). After the discretization of the domain, the soil properties were generated using random field theory explained in section 4. The LB method was employed to solve the mass transfer equation. The Neumann boundary condition was assumed for the borders of the domain excluding line MN. Both grid size and time step play key parts in the stability, convergence, and the accuracy of numerical solutions. Following numerous numerical tests, the grid size was set to 0.5 m. The time step was chosen for each realization according to the stable domain presented in Fig. 1. Consequently, the time step varied between 0.5 to 4 min based on the range of variables in every realization.

In case where the stochastic parameters mentioned above are constant in the whole domain, the analytical solution of the advection-reaction-dispersion equation (Eq. (1)) is stated as Eq. (20) [49]:

$$C(x,y,t) = C_0 \sum_{n=0}^{\infty} L_n P_n \cos(\eta y)$$
$$\cdot\left\{\exp\left(\frac{x(U-\beta)}{2D}\right)\operatorname{erfc}\left(\frac{x-\beta t}{2\sqrt{D\,t}}\right) + \exp\left(\frac{x(U+\beta)}{2D}\right)\operatorname{erfc}\left(\frac{x+\beta t}{2\sqrt{D\,t}}\right)\right\}$$
$$L_n = \begin{cases} 0.5 & n = 0 \\ 1 & n > 0 \end{cases}$$
$$P_n = \begin{cases} \dfrac{Y_2 - Y_1}{W} & n = 0 \\ \dfrac{[\sin(\eta Y_2) - \sin(\eta Y_1)]}{n\pi} & n > 0 \end{cases} \qquad (20)$$
$$\eta = n\pi / W \qquad n = 0,\ 1,\ 2,\ 3,\ \ldots$$
$$\beta = \sqrt{U^2 + 4D_x(\eta^2 D_y + \lambda)}$$

where Y_1 and Y_2 are transversal locations of input pollution plume (see Fig. 2) and W is domain width.

6.2. Problem 2

This problem is also a two-dimensional mass transfer problem where point source pollution enters the domain. The pollution plume with the rate of 43 mg/min enters the groundwater at Point F (Fig. 2b). The domain size, the initial and boundary conditions, and the stochastic parameters are identical to assumptions mentioned in problem 1. The numerical solution for this problem is available in the literature [50].

7. Results and discussion

7.1. Deterministic analysis

Aiming to check the accuracy of the LB method, the numerical solutions were verified with the analytical answers for the above-mentioned 2D mass transfer problems. According to Fig. 3, both numerical and analytical solutions give identical time-concentration curves at point P (see Fig. 2). Here, $\lambda = 0.0005$ 1/min, D=0.003 m^2/min, U=0.03 m/min, dx=1 m, dt=2 min. The high level of agreement is also observed in the concentration contour lines at steady state (Fig. 3), confirming the high precision of the presented numerical code.

7.2. Effects of spatial variability of dispersion coefficient

Fig. 4 shows the spatial variability of the dispersion coefficient in different autocorrelation distances of 1 and 10 m, respectively. The coefficient of variations in these figures is 0.5. As shown, the higher the autocorrelation distance is, the more homogeneous soil realization is obtained.

Regarding problem 1, Figs. 5a and 5b show the effects of spatial variability of the dispersion coefficient on the mean of mass travel time when the concentration is equal to 5 and 20 mg/lit, i.e. $T_{c=5}$ and $T_{c=20}$, respectively. Several values of COV and autocorrelation distance were taken into consideration. Accordingly, $T_{c=5}$ increased and $T_{c=20}$ decreased with a rise in the value of COV in all autocorrelation distances. The highest $T_{c=5}$ was obtained when the autocorrelation distance was 1 m, while the highest $T_{c=20}$ was attained at an autocorrelation distance of 20 m. In addition, the mean of mass travel time was more affected by COV of dispersion coefficient in comparison to autocorrelation distance of that coefficient. For instance, considering the autocorrelation distance of 10 m, $T_{c=5}$ varied from 1240 to 1259 min when the COV increased from 0.125 to 1, representing 1.5% variation in the mean travel time. Nevertheless, $T_{c=5}$ ranged from 1259 to 1262 min for different autocorrelation distances at COV= 1, indicating 0.2% increase in $T_{c=5}$.

The effects of spatial variability on the standard deviation of $T_{c=5}$ and $T_{c=20}$ for problem 1 are also shown in Fig. 5. Accordingly, the standard deviation is constantly increasing with an increase in the values of COV and autocorrelation distance, implying that wider histograms are obtained for $T_{c=5}$ and $T_{c=20}$ at greater COV and autocorrelation distances.

Besides, the cumulative distribution functions (CDF) of $T_{c=5}$ for several autocorrelation distances are displayed in Fig. 6a. Interestingly, all CDF curves intersect neatly at the same point. Accordingly, the probability that $T_{c=5}$ is less than 1250 min is about 52 % regardless of different autocorrelation distances, i.e., $P(T_{c=5} < 1250\,\text{min}) = 0.52$. Two types of behavior are perceived from Fig. 6a regarding the values of $T_{c=5}$ higher or smaller than 1250 min. Considering higher values of $T_{c=5}$, the cumulative probability decreases with a rise in autocorrelation distance, and vice-versa for smaller values of $T_{c=5}$. Similarly, the crossing of CDF curves of $T_{c=5}$ for a number of COV values at approximately one point is also observed (Fig. 6b). In these cases, $P(T_{c=5} < 1230\ \text{min})$ is 40 % irrespective of the COV values.

It is worth mentioning that the probability distributions of $T_{c=5}$ are accurately described with normal, lognormal, and skew normal distributions. In line with Table 2, the correlation coefficients between the histograms and the induced distributions are higher than 0.98, signifying the high level of compliance. Several values of COV and autocorrelation distances are considered in the above evaluation, as reported in Table 2.

Figs. 6c and 6d show the influence of stochastic dispersion coefficient on the mean time-concentration curves for problem 1, considering several values of COV and different autocorrelation distances. Regarding different values of COV, the time-concentration curves are closely in agreement at early times, while the final mean concentrations are slightly different, ranging from 36 to 40 mg/lit (Fig 6c). The final mean concentration increases once the COV of dispersion coefficient rises. Therefore, a greater portion of mass is transported longitudinally at higher COV values for dispersion coefficient, and consequently a smaller portion leaves the domain transversally. Concerning various autocorrelation distance, the breakthrough curves are in high agreement, which confirms that the autocorrelation distance is insignificant (Fig 6d).

In terms of problem 2, the influences of spatial variability of dispersion coefficient on the mean and standard deviation of $T_{c=5}$ and $T_{c=20}$ are shown in Fig. 7. Similar to results presented in Fig. 5, there are upward and downward trends in the mean values of $T_{c=5}$ and $T_{c=20}$, respectively, with a rise in the value of COV. In line with Fig. 7a, $T_{c=5}$ increases approximately from 941 to 953 min once the COV varies from 0.125 to 1, Indicating 1.3 % variation in the mean travel time. Moreover, the standard deviations of both $T_{c=5}$ and $T_{c=20}$ increase with COV values, which are in accordance with the increasing trends in Figs. 5c and 5d. Analogous to problem 1, the CDF curves of $T_{c=5,}$ which stemmed from numerous COV values or those resulted from several autocorrelation distances, intersect approximately at the same point. For instance, the CDF curves of Tc=5, stemmed from several COV and the autocorrelation distance of 5 m, intersect approximately at the cumulative probability of 46% ($P(T_{c=5} < 939 \text{ min}) = 46\%$).

The results mentioned above indicate that the stochastic dispersion coefficient ends up with small variations in the mean of mass travel time and the time-concentration curves. The stochastic concentration contour lines of several realizations with regards to spatial variability of dispersion coefficient for both problems are shown in Fig. 8. It is observed that the concentration contour lines deviated slightly in different directions.

7.3. Effects of spatial variability of pore velocity

The influence of inherent uncertainty of pore velocity on the mass transfer is also explored. Concerning problem 1, Fig. 9 shows an increase in the mean and standard deviation of $T_{c=5}$ versus COV for different autocorrelation distances. According to Fig. 9a, the mean of $T_{c=5}$ changes considerably with respect to the COV of pore velocity. For instance, considering autocorrelation distance of 10 m, the mean of $T_{c=5}$ ranges from 1247 to 1755 min when the COV varies from 0.125 to 1, indicating 41 % increase in the mean travel time. Compared to the results obtained from spatial variability of dispersion coefficient (see Fig. 5a), the mean of mass travel time is much more sensitive to the COV of pore velocity. Besides, the standard deviation of $T_{c=5}$ varies between 83 to 605 min (Fig. 9b), which is nearly 10 times higher than the range of standard deviation obtained from spatial variability of dispersion coefficient (see Fig. 5b).

In addition, the mean and standard deviation of $T_{c=5}$ rises with an increase in the autocorrelation distance. The estimated mean of $T_{c=5}$ varies between 1382 and 1756 min with regard to COV=1, representing 27% increase in $T_{c=5}$ (see Fig. 9). Therefore, the role of autocorrelation distance is significant in the mass transfer once the velocity is considered to comply as a random field variable. It should be pointed out that similar figures were perceived for greater travel times, which are not offered here for the sake of brevity.

Of note, the lognormal distribution, followed by skew normal distribution, gives the best fit to the histograms of $T_{c=5}$ (Table 3). The R^2 values higher than 0.95 confirm these good agreements. Regarding numerous values of COV for velocity, all CDF curves approximately cross each other when $T_{c=5}$=1150 min (Figs. 10a). Furthermore, the CDF curves of $T_{c=5}$, stemming from different autocorrelation distances for velocity, intersect each other at the same point (Fig. 10b). The slope of CDF curves is affected noticeably by the values of autocorrelation distance. In line with Fig. 10b, the cumulative probability of $T_{c=5}$ increases with respect to autocorrelation distance when $T_{c=5}$<1240 min, whereas that probability declines once $T_{c=5}$>1240 min.

The mean breakthrough curves at point P (see Fig. 2) when the velocity is considered as a random field variable are also depicted in Fig. 10. The slope of breakthrough curves is influenced considerably by the variations in the values of COV. Accordingly, the mean concentrations of mass at termination times are in the range of 21 to 36 mg/lit. Remarkably, the minimum concentration is attained at the greatest value of COV. The reason being that the likelihood of

small velocities in the domain is high when the COV of velocity is large. Consequently, points with small velocities act as obstacles against mass transfer alongside x direction, resulting in less longitudinal mass transport. In other word, a larger portion of pollution is transported in lateral direction through the dispersion phenomenon at greater COV values.

Regarding the effects of autocorrelation distance on the breakthrough curves, the final mean concentrations of mass at the small autocorrelation distances are considerably higher than those resulted from large autocorrelation distances. The clue to this observation may be the fact that the region is more homogeneous when the autocorrelation distance is large.

According to results obtained for problem 2, the mean and standard deviation of $T_{c=5}$ manifests a considerable increasing trend with respect to both COV and autocorrelation distance (Fig. 11). For instance, the mean of $T_{c=5}$ changes between 950 and 1310 min for the autocorrelation distance of 20 m, which indicates roughly 38 % alteration. These results confirm that the variability of pore velocity influences the mass transfer phenomenon considerably. It was also observed that the CDF curves cross roughly at an identical point. In the case where the autocorrelation distance is equal to 5 m, the probability that $T_{c=5}$ is smaller than 901 min is equal to 30 %, considering all COV values.

7.4. Effects of spatial variability of reaction term

To explain the effect of reaction term (λ) on mass transfer, the time-concentration curves of advection dispersion equation with and without λ are illustrated in Fig. 12, considering problem 1. As shown, the final mass concentration declined over 50% by considering the reaction rate of $\lambda = 0.0005\ (1/\min)$. Moreover, the slope of time-concentration curve decreased by the implementation of reaction term. The reason being that the mass is decayed in the domain by considering the reaction term.

The influence of spatial variability for reaction term in the transport equation (Eq. (1)) is given in Fig. 13. Two types of behavior are perceived for the mean value of $T_{c=5}$. The mean of $T_{c=5}$ tends to fall behind the deterministic value ($T_{c=5}$=1239 min) for the autocorrelation distances of 1, 2, 5 m, while this parameter increases at autocorrelation distances larger than 5 m. Nonetheless, standard deviation of $T_{c=5}$ increases with elevation of both autocorrelation distance and COV

values. It should be pointed out that the variations of $T_{c=5}$ are limited. According to Fig. 13a, $T_{c=5}$ changes between 1238 and 1244 min at different values of COV and autocorrelation distance, indicating 0.5 % variation of $T_{c=5}$. Therefore, the probabilistic assumption for reaction term causes negligible influence on the mass transfer.

Furthermore, the time-concentration and CDF curves for different values of autocorrelation distance and COV are displayed in Fig. 14. The slope of time-concentration curves is not influenced by the variations of COV and autocorrelation distance. In addition, the terminal concentration varies slightly at various values of COV and autocorrelation distance. These results indicated that the stochastic variations of reaction term cause small effects on the mass transfer. However, the presence of reaction term in the advection dispersion equation declines the final concentration considerably.

In these cases, where the reaction term is a random field variable, the skew normal distribution ends up with high accordance with the histograms of $T_{c=5}$. However, based on the R^2 values given in Table 4, both normal and lognormal distributions may explain the histograms satisfactorily. Similar to Figs. 6 and 10, the CDF curves of $T_{c=5}$, arisen from several values of autocorrelation distance or COV, meet each other nearly at identical point (Fig. 14). The slope of CDF curves declines with an increase in the values of COV and autocorrelation distance.

The mean of $T_{c=5}$ reflects a tendency to decrease with COV at small autocorrelation distances, considering the results of problem 2 (Fig. 15). Besides, the mean of $T_{c=5}$ is between 940 and 942 at different values of COV and autocorrelation distance, indicating 0.2 % deviation which corroborates insignificant effects of probabilistic reaction term for mass transfer in problem 2. Regarding the standard deviation of $T_{c=5}$, the increasing trend with respect to both COV and autocorrelation distance is observed in Fig. 15. Akin to previous cases, the intersection of CDF curves at an approximately identical point is perceived.

7.5. Effect of cross-correlation between dispersion coefficient and pore velocity

The effects of cross-correlation coefficient between D and U on the mean of $T_{c=5}$ are illustrated in Fig. 16. Both dispersion coefficient and pore velocity are considered as random field variables with the COV of 0.25. This figure is obtained for problem 1. Accordingly, with an increase in

correlation coefficient, a higher mean of mass travel time ($T_{c=5}$) is estimated for different autocorrelation distances. For instance, the mean of $T_{c=5}$ varies from 1267 to 1280 min when the correlation coefficient between D and U increases from 0.1 to 0.9, considering the autocorrelation distance of 5 m. The interpretation is that D and U are linearly more dependent on one another at greater cross-correlation coefficients. At lower cross-correlation coefficients, there are numerous realizations where velocity is small, whereas the dispersion is high. However, at higher cross-correlation coefficients, the simultaneous occurrence of smaller D and U values is more plausible. Therefore, longer elapsed time is needed at smaller correlation coefficient for the pollution to reach the end point P. In addition, the standard deviation of $T_{c=5}$ increases slightly with a rise in the cross-correlation coefficient between dispersion coefficient and pore velocity (see Fig. 16).

In addition, the values of correction for the cross-correlation coefficient (F) are given in Table 5. The correction coefficient, F, changes from 1.003 to 1.027, whereby the maximum F is associated with the smallest cross-correlation coefficient. Furthermore, this coefficient decreases noticeably when the cross-correlation coefficient increases. The results indicated that the implementation of correction coefficient leads to negligible influences on the results presented in Fig. 16.

8. Conclusion

In this study, the two-dimensional mass transfer problem was probabilistically analyzed and the influences of uncertainty in the parameters of advection-reaction-dispersion equation were explored. The results indicated that the combination of the lattice Boltzmann method and random field generation can be employed to successfully consider the effect of spatial variability in parameters associated with advection-reaction-dispersion equation.

Amongst the spatial variability of dispersion coefficient, reaction term, and pore velocity, the latter was most influential on the variations of mass travel time and time-concentration curve at the termination point. Considering large values of COV for pore velocity, higher rate of mass was transported in lateral direction. However, the spatial variability of dispersion coefficient caused slight changes in the mean of mass travel time and the time-concentration curve. Although the existence of reaction term in the advection-dispersion equation changed the terminal mass

concentration noticeably, its spatial variability ended up with small variations on the mass transfer process. Considering all stochastic parameters, the CDF curves of mass travel time ($T_{c=5}$), stemmed from several autocorrelation distances or various values of COV, intersect neatly at the same point. Finally, several cross-correlation coefficients were assumed between the random field of dispersion coefficient and the realizations of pore velocity. It was observed that the mean travel time increases at higher values of cross-correlation coefficient.

References

[1] T. Nazir, M. Abbas, A.I.M. Ismail, A.A. Majid, A. Rashid, The numerical solution of advection–diffusion problems using new cubic trigonometric B-splines approach, Applied Mathematical Modelling, 40(7-8) (2016) 4586-4611.

[2] L. Shi, L. Zeng, Y. Tang, C. Chen, J. Yang, Uncertainty quantification of contaminant transport and risk assessment with conditional stochastic collocation method, Stochastic environmental research and risk assessment, 27(6) (2013) 1453-1464.

[3] J.C. Cortés, A. Navarro-Quiles, J.V. Romero, M.D. Roselló, M.A. Sohaly, Solving the random Cauchy one-dimensional advection–diffusion equation: Numerical analysis and computing, Journal of Computational and Applied Mathematics, 330 (2018) 920-936.

[4] A. Fiori, A. Zarlenga, I. Jankovic, G. Dagan, Solute transport in aquifers: The comeback of the advection dispersion equation and the First Order Approximation, Advances in Water Resources, 110 (2017) 349-359.

[5] J. Li, J. Jagalur-Mohan, A.A. Oberai, O. Sahni, Stochastic variational multiscale analysis of the advection–diffusion equation: Advective–diffusive regime and multi-dimensional problems, Computer Methods in Applied Mechanics and Engineering, 325 (2017) 766-799.

[6] S. Chakraverty, B. Sahoo, T. Rao, P. Karunakar, B. Sapra, Modelling uncertainties in the diffusion-advection equation for radon transport in soil using interval arithmetic, Journal of environmental radioactivity, 182 (2018) 165-171.

[7] D. Griffiths, J. Huang, G.A. Fenton, Probabilistic infinite slope analysis, Computers and Geotechnics, 38(4) (2011) 577-584.

[8] M. Lo, Y. Leung, Probabilistic analyses of slopes and footings with spatially variable soils considering cross-correlation and conditioned random field, Journal of Geotechnical and Geoenvironmental Engineering, 143(9) (2017) 04017044.

[9] S.E. Cho, Probabilistic analysis of seepage that considers the spatial variability of permeability for an embankment on soil foundation, Engineering Geology, 133 (2012) 30-39.
[10] X. Tan, X. Wang, S. Khoshnevisan, X. Hou, F. Zha, Seepage analysis of earth dams considering spatial variability of hydraulic parameters, Engineering Geology, 228 (2017) 260-269.
[11] A.A. Hekmatzadeh, F. Zarei, A. Johari, A. Torabi Haghighi, Reliability analysis of stability against piping and sliding in diversion dams, considering four cutoff wall configurations, Computers and Geotechnics, 98 (2018) 217-231.
[12] A. Srivastava, G.S. Babu, S. Haldar, Influence of spatial variability of permeability property on steady state seepage flow and slope stability analysis, Engineering Geology, 110(3-4) (2010) 93-101.
[13] A.A. Ahmed, Stochastic analysis of free surface flow through earth dams, Computers and Geotechnics, 36(7) (2009) 1186-1190.
[14] A.A. Ahmed, Stochastic analysis of seepage under hydraulic structures resting on anisotropic heterogeneous soils, Journal of Geotechnical and Geoenvironmental Engineering, 139(6) (2012) 1001-1004.
[15] G.A. Fenton, D. Griffiths, Extreme hydraulic gradient statistics in stochastic earth dam, Journal of geotechnical and geoenvironmental engineering, 123(11) (1997) 995-1000.
[16] D. Griffiths, G.A. Fenton, Seepage beneath water retaining structures founded on spatially random soil, Geotechnique, 43(4) (1993) 577-587.
[17] D. Griffiths, G.A. Fenton, Three-dimensional seepage through spatially random soil, Journal of geotechnical and geoenvironmental engineering, 123(2) (1997) 153-160.
[18] D. Griffiths, G.A. Fenton, Probabilistic analysis of exit gradients due to steady seepage, Journal of Geotechnical and Geoenvironmental Engineering, 124(9) (1998) 789-797.
[19] D.M. Do, W. Gao, C. Song, Stochastic finite element analysis of structures in the presence of multiple imprecise random field parameters, Computer Methods in Applied Mechanics and Engineering, 300 (2016) 657-688.
[20] K. Wang, G. Huang, Effect of permeability variations on solute transport in highly heterogeneous porous media, Advances in Water Resources, 34(6) (2011) 671-683.
[21] H. Baalousha, J. Köngeter, Stochastic modelling and risk analysis of groundwater pollution using FORM coupled with automatic differentiation, Advances in water resources, 29(12) (2006) 1815-1832.
[22] D.K. Green, Efficient Markov Chain Monte Carlo for combined Subset Simulation and nonlinear finite element analysis, Computer Methods in Applied Mechanics and Engineering, 313 (2017) 337-361.
[23] D.V. Griffiths, G.A. Fenton, Probabilistic Slope Stability Analysis by Finite Elements, Journal of Geotechnical and Geoenvironmental Engineering, 130(5) (2004) 507-518.

[24] C. Zheng, G.D. Bennett, Applied contaminant transport modeling, Wiley-Interscience New York, 2002.

[25] Y. Lian, Y. Ying, S. Tang, S. Lin, G.J. Wagner, W.K. Liu, A Petrov–Galerkin finite element method for the fractional advection–diffusion equation, Computer Methods in Applied Mechanics and Engineering, 309 (2016) 388-410.

[26] A. Hekmatzadeh, H. Keshavarzi, N. Talebbeydokhti, A. Torabi Haghighi, Lattice Boltzmann solution of advection-dominated mass transport problem: a comparison, Scientia Iranica, (2018).

[27] J. Perko, R.A. Patel, Single-relaxation-time lattice Boltzmann scheme for advection-diffusion problems with large diffusion-coefficient heterogeneities and high-advection transport, Physical Review E, 89(5) (2014) 053309.

[28] Q. Kang, P.C. Lichtner, M. Ehrhardt, A lattice Boltzmann method for coupled fluid flow, solute transport, and chemical reaction, Progress in Computational Physics Volume 3: Novel Trends in Lattice-Boltzmann Methods, 3 (2013) 184.

[29] B. Servan-Camas, F.T.-C. Tsai, Lattice Boltzmann method with two relaxation times for advection–diffusion equation: third order analysis and stability analysis, Advances in Water Resources, 31(8) (2008) 1113-1126.

[30] K.V. Sharma, R. Straka, F.W. Tavares, New Cascaded Thermal Lattice Boltzmann Method for simulations of advection-diffusion and convective heat transfer, International Journal of Thermal Sciences, 118 (2017) 259-277.

[31] B. Servan-Camas, F.T.-C. Tsai, Non-negativity and stability analyses of lattice Boltzmann method for advection–diffusion equation, Journal of Computational Physics, 228(1) (2009) 236-256.

[32] A. Xu, L. Shi, T. Zhao, Accelerated lattice Boltzmann simulation using GPU and OpenACC with data management, International Journal of Heat and Mass Transfer, 109 (2017) 577-588.

[33] A. Xu, W. Shyy, T. Zhao, Lattice Boltzmann modeling of transport phenomena in fuel cells and flow batteries, Acta Mechanica Sinica, 33(3) (2017) 555-574.

[34] J. Ji, C. Zhang, Y. Gao, J. Kodikara, Effect of 2D spatial variability on slope reliability: A simplified FORM analysis, Geoscience Frontiers, (2017).

[35] S.-H. Jiang, D.-Q. Li, Z.-J. Cao, C.-B. Zhou, K.-K. Phoon, Efficient System Reliability Analysis of Slope Stability in Spatially Variable Soils Using Monte Carlo Simulation, Journal of Geotechnical and Geoenvironmental Engineering, 141(2) (2015) 04014096.

[36] N. Suciu, Diffusion in random velocity fields with applications to contaminant transport in groundwater, Advances in water resources, 69 (2014) 114-133.

[37] N. Suciu, F.A. Radu, A. Prechtel, F. Brunner, P. Knabner, A coupled finite element–global random walk approach to advection-dominated transport in porous media with random hydraulic conductivity, Journal of Computational and Applied Mathematics, 246 (2013) 27-37.
[38] K. Zhang, H. Li, G. Achari, Fuzzy-stochastic characterization of site uncertainty and variability in groundwater flow and contaminant transport through a heterogeneous aquifer, Journal of contaminant hydrology, 106(1-2) (2009) 73-82.
[39] H. Zhang, C. Misbah, Lattice Boltzmann simulation of advection-diffusion of chemicals and applications to blood flow, Computers & Fluids, 187 (2019) 46-59.
[40] M. Mozafari-Shamsi, M. Sefid, G. Imani, Application of the ghost fluid lattice Boltzmann method to moving curved boundaries with constant temperature or heat flux conditions, Computers & Fluids, 167 (2018) 51-65.
[41] Z. Cao, Y. Wang, Bayesian model comparison and selection of spatial correlation functions for soil parameters, Structural Safety, 49 (2014) 10-17.
[42] G.B. Baecher, J.T. Christian, Reliability and statistics in geotechnical engineering, John Wiley & Sons, 2005.
[43] D. Griffiths, G.A. Fenton, Probabilistic settlement analysis by stochastic and random finite-element methods, Journal of geotechnical and geoenvironmental engineering, 135(11) (2009) 1629-1637.
[44] D.-Q. Li, S.-H. Jiang, Z.-J. Cao, W. Zhou, C.-B. Zhou, L.-M. Zhang, A multiple response-surface method for slope reliability analysis considering spatial variability of soil properties, Engineering Geology, 187 (2015) 60-72.
[45] M. Papadrakakis, N.D. Lagaros, Reliability-based structural optimization using neural networks and Monte Carlo simulation, Computer methods in applied mechanics and engineering, 191(32) (2002) 3491-3507.
[46] A. Johari, S. Hosseini, A. Keshavarz, Reliability analysis of seismic bearing capacity of strip footing by stochastic slip lines method, Computers and Geotechnics, 91 (2017) 203-217.
[47] A. Der Kiureghian, P.-L. Liu, Structural reliability under incomplete probability information, Journal of Engineering Mechanics, 112(1) (1986) 85-104.
[48] J. Yang, Z.-Y. Yin, F. Laouafa, P.-Y. Hicher, Analysis of suffusion in cohesionless soils with randomly distributed porosity and fines content, Computers and Geotechnics, 111 (2019) 157-171.
[49] E.J. Wexler, Analytical solutions for one-, two-, and three-dimensional solute transport in ground-water systems with uniform flow, US Government Printing Office, 1992.
[50] R. Charbeneau, S. Sherif, Groundwater Hydraulics and Pollutant Transport, Applied Mechanics Reviews, 55 (2002) B38.

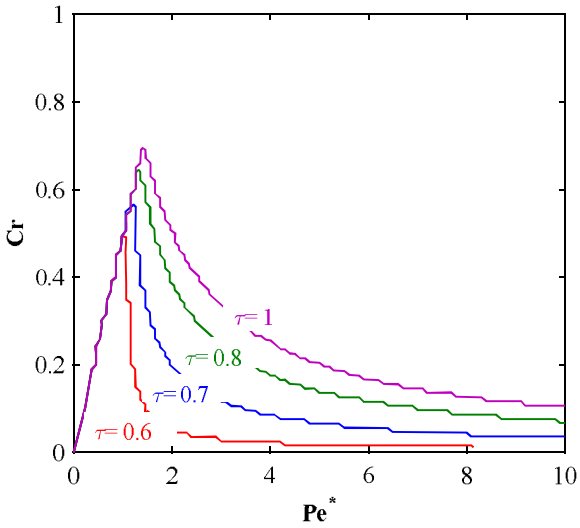

Fig. 1. Stability domain for D2Q5 lattices. The stable domain is the area underneath the solid lines. Redrawn after [31].

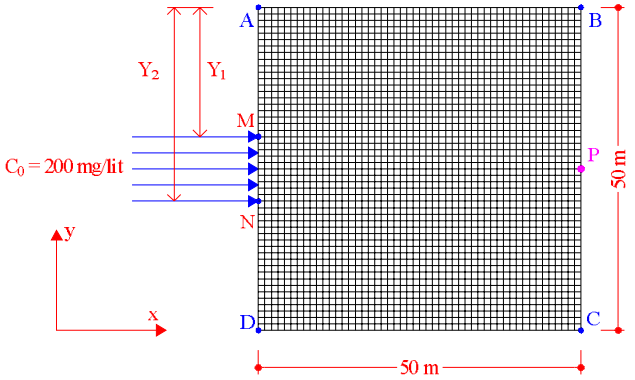

(a)

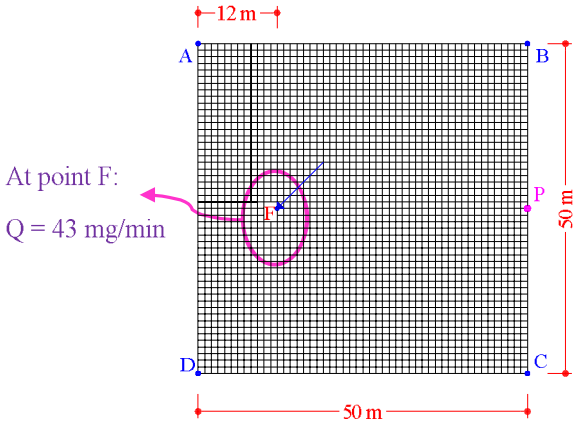

(b)

Fig. 2. Characteristics of the mass transfer problems. (a) problem 1, (b) problem 2.

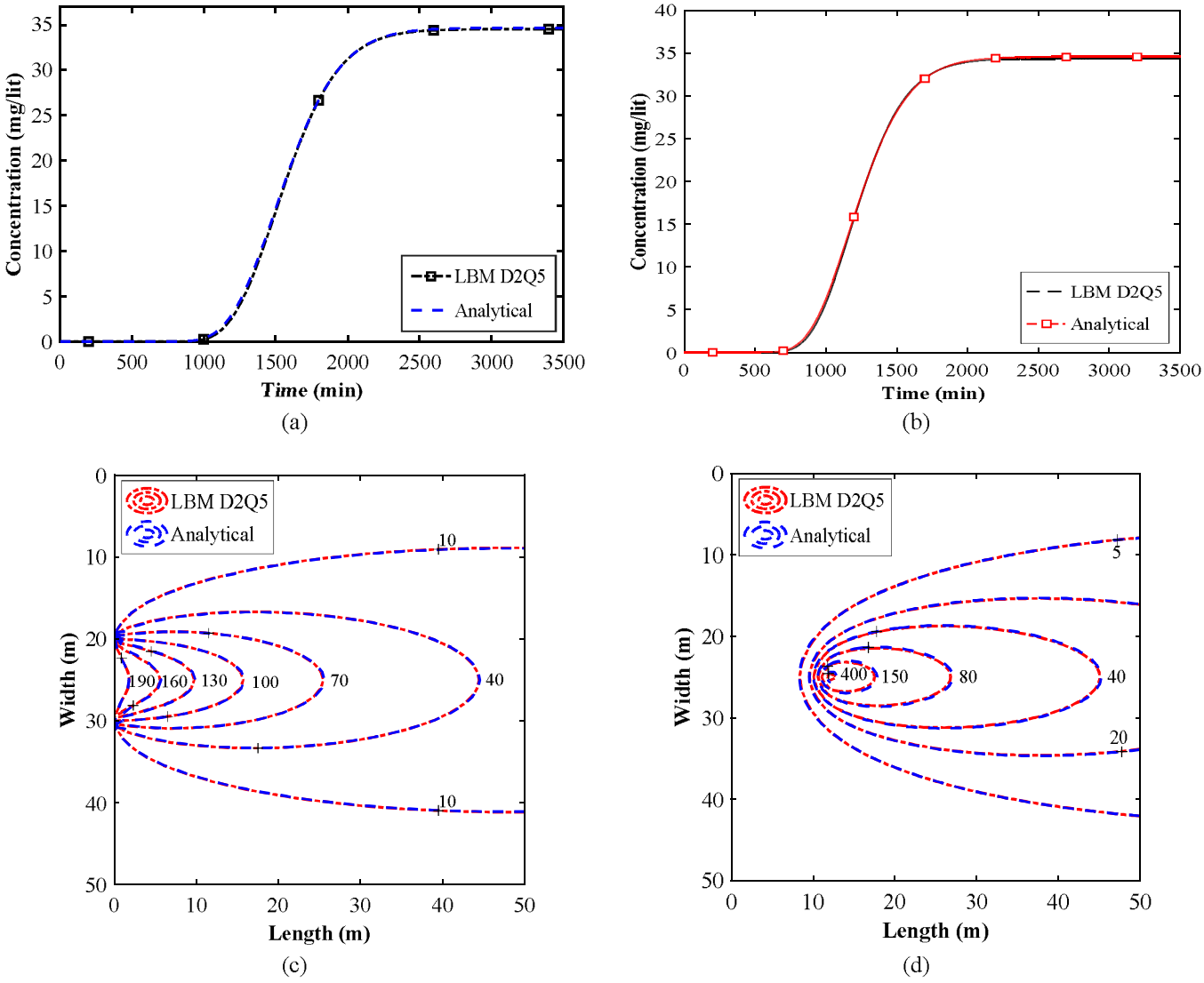

Fig. 3. Comparison of numerical and analytical solutions. (a) time-concentration curves of problem 1, (b) time-concentration curves of problem 2, (c) concentration counters of problem 1, (d) concentration counters of problem 2.

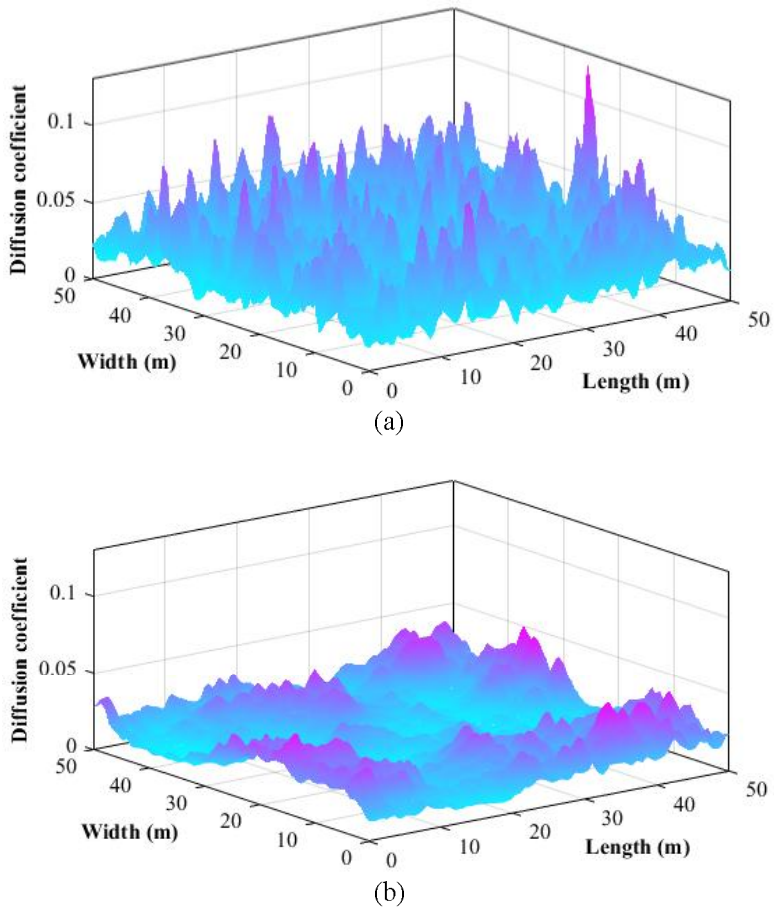

Fig. 4. Typical realizations of random field for the dispersion coefficient at two autocorrelation distances. (a) autocorrelation distance equals to 1m, (b) autocorrelation distance equals to 10 m.

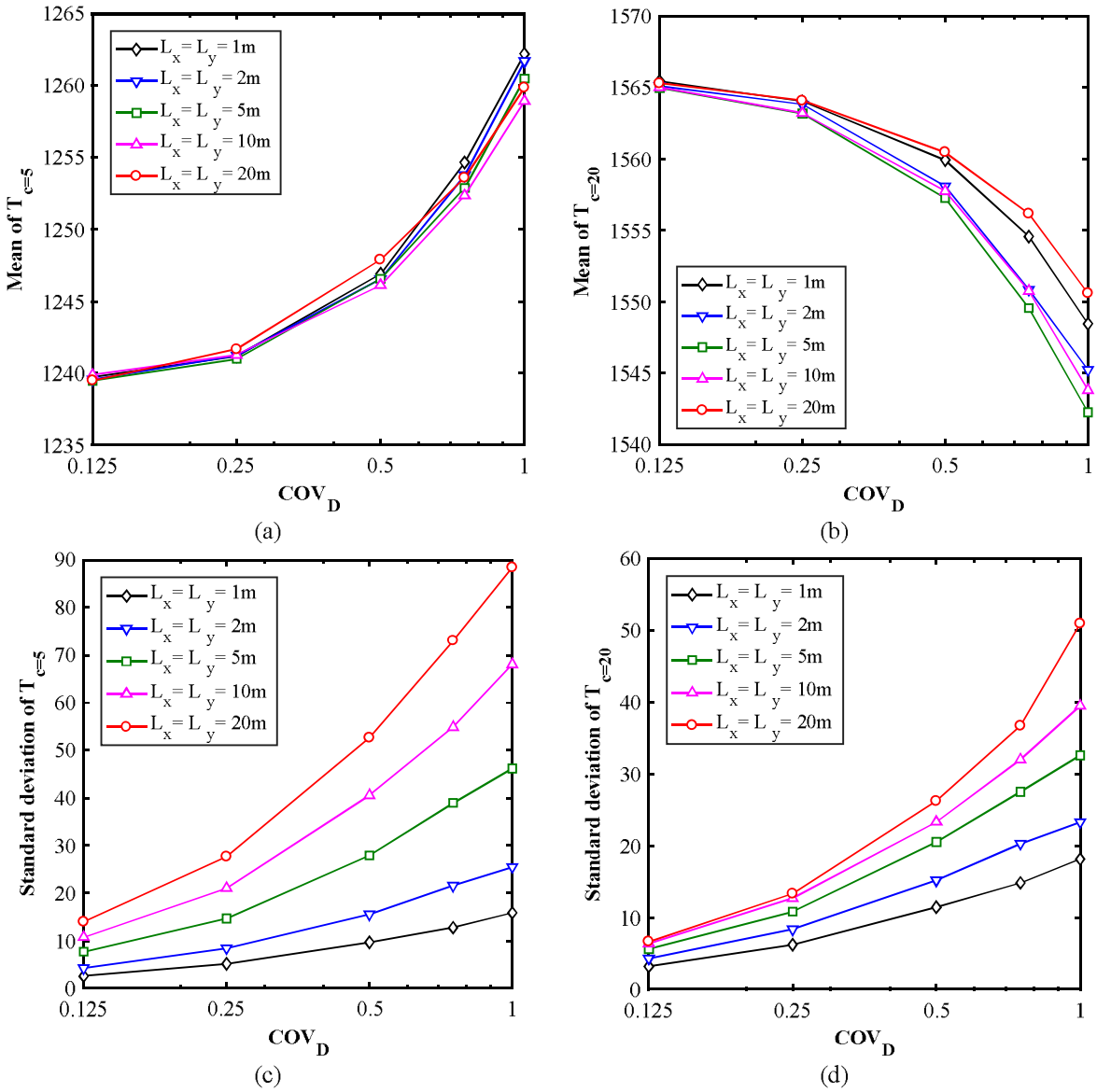

Fig. 5. Influence of COV and autocorrelation distance for the dispersion coefficient on the mass travel time in problem 1. (a) mean of $T_{c=5}$, (b) mean of $T_{c=20}$, (c) standard deviation of $T_{c=5}$, (d) standard deviation of $T_{c=20}$.

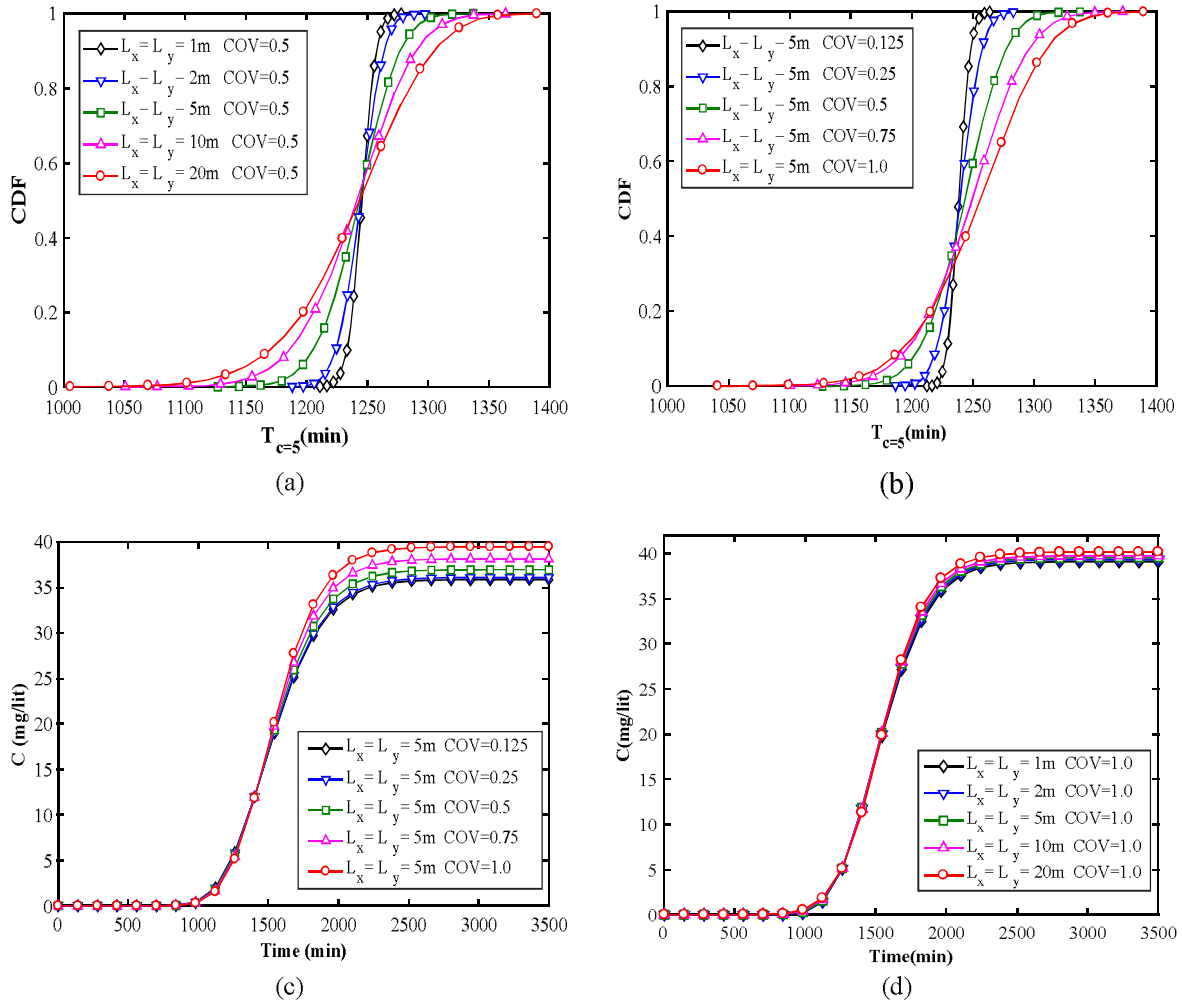

Fig. 6. Influence of stochastic dispersion coefficient on the CDF and mean time-concentration curves in problem 1. (a) CDF curves of $T_{c=5}$ obtained from different autocorrelation distances, (b) CDF curves of $T_{c=5}$ obtained from different COV values, (c) time-concentration curves resulted from different COV values, (d) time-concentration curves resulted from different autocorrelation distances.

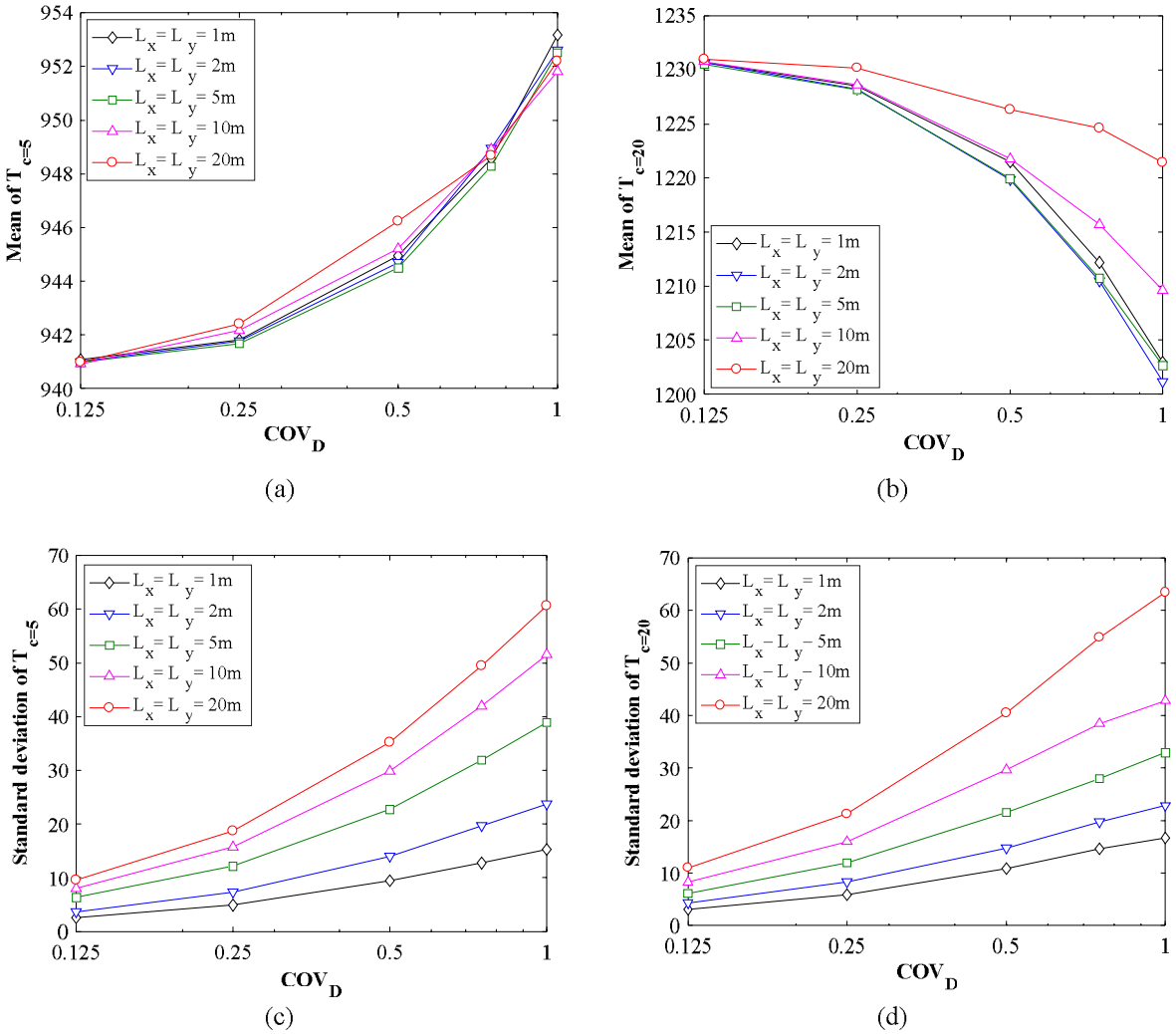

Fig. 7. Influence of COV and autocorrelation distance for the dispersion coefficient on the mass travel time in problem 2. (a) mean of $T_{c=5}$, (b) mean of $T_{c=20}$, (c) standard deviation of $T_{c=5}$, (d) standard deviation of $T_{c=20}$.

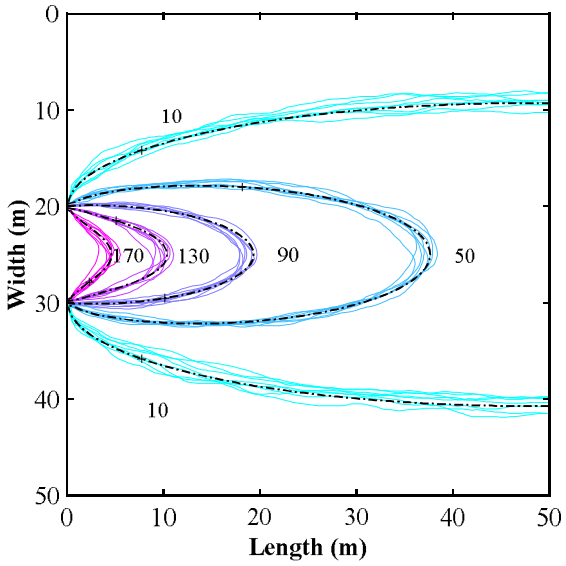

(a)

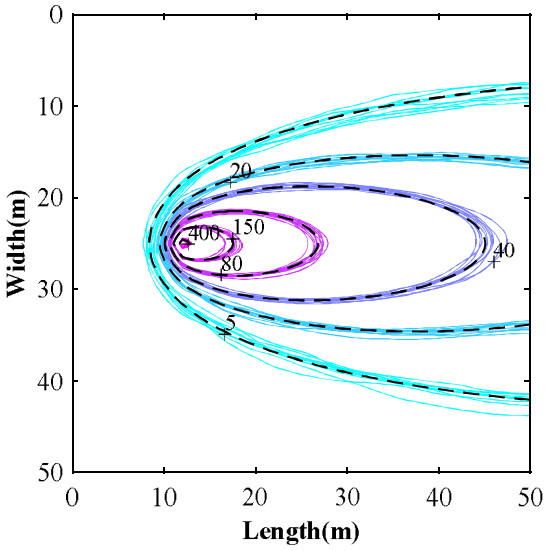

(b)

Fig. 8. Stochastic and deterministic concentration counters, considering stochastic dispersion. (a) problem 1, (b) problem 2.

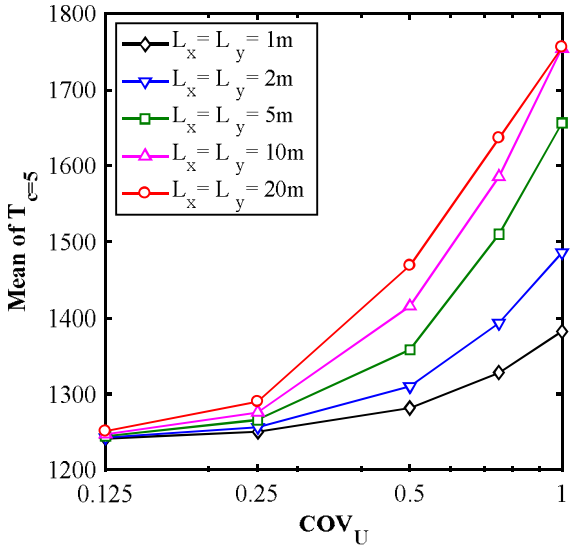

(a)

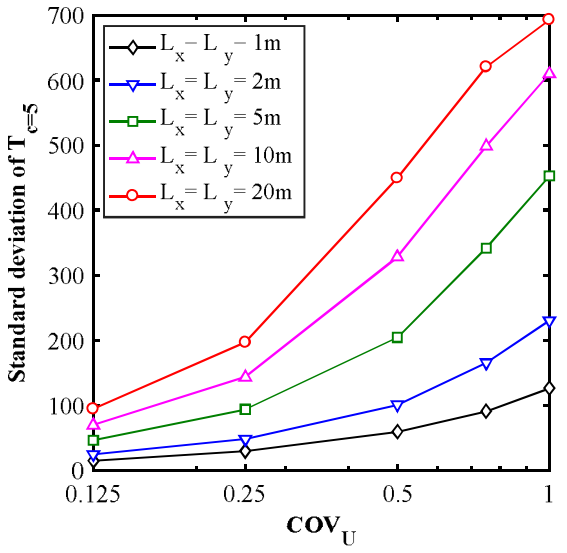

(b)

Fig. 9. Influence of COV and autocorrelation distance for the pore velocity on the mass travel time in problem 1. (a) mean of $T_{c=5}$, (b) standard deviation of $T_{c=5}$.

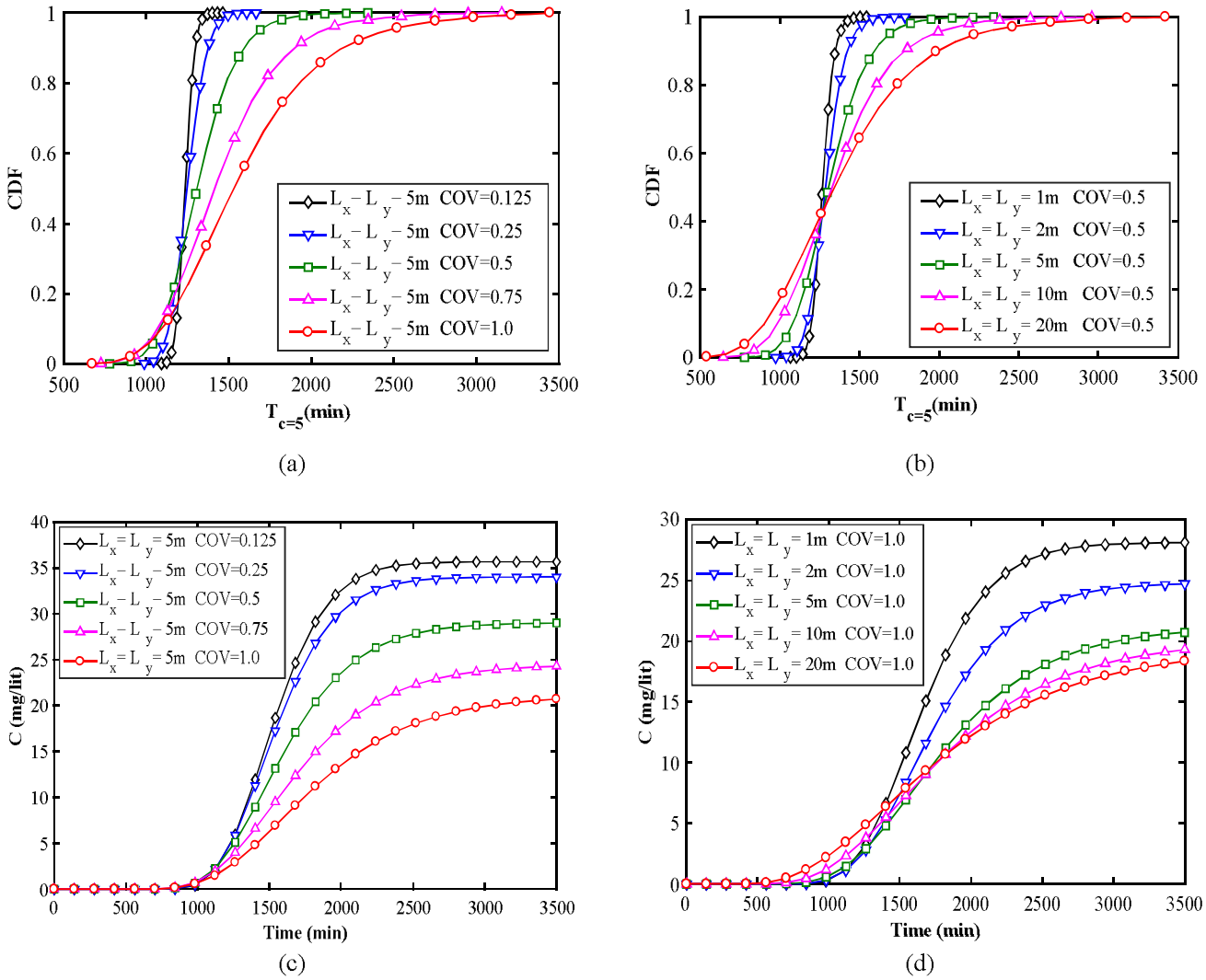

Fig. 10. Influence of stochastic pore velocity on the CDF and mean time-concentration curves in problem 1. (a) CDF curves of $T_{c=5}$ obtained from different COV values, (b) CDF curves of $T_{c=5}$ obtained from different autocorrelation distances, (c) time-concentration curves resulted from different COV values, (d) time-concentration curves resulted from different autocorrelation distances.

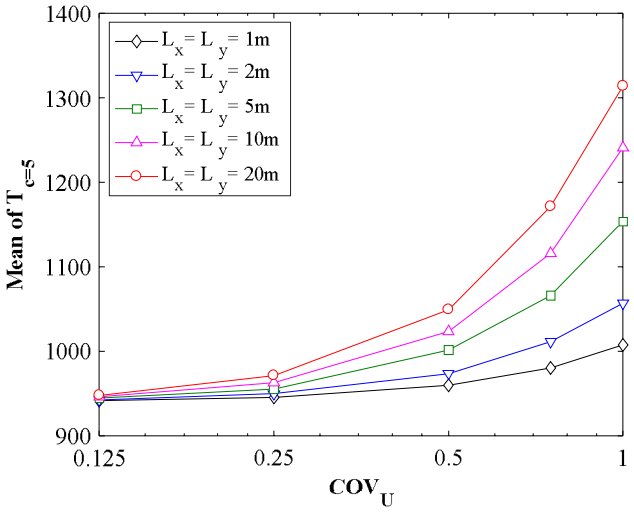

(a)

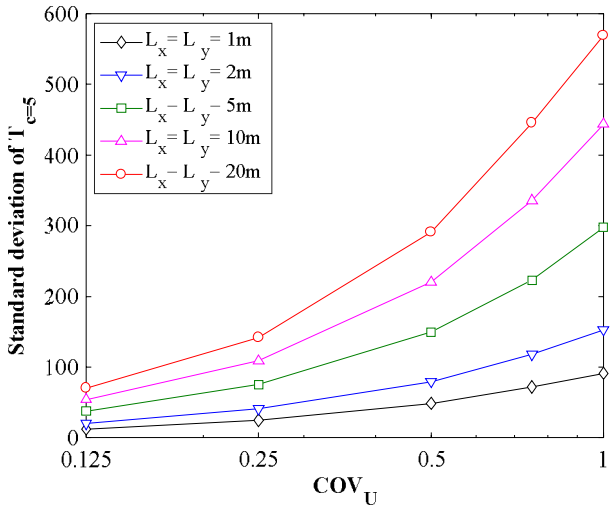

(b)

Fig. 11. Influence of COV and autocorrelation distance for the pore velocity on the mass travel time in problem 2. (a) mean of Tc=5, (b) standard deviation of Tc=5.

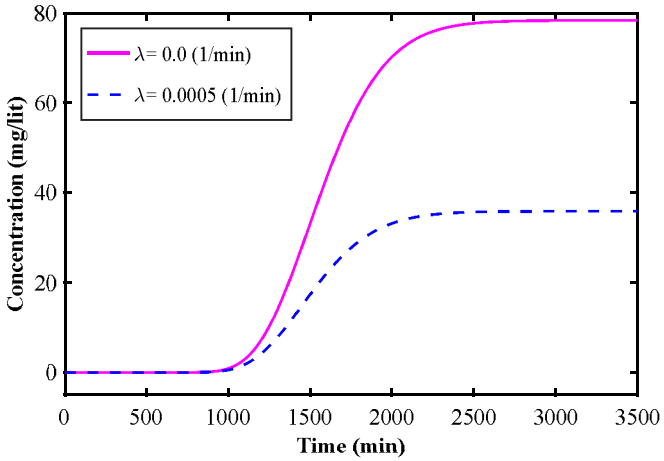

Fig. 12. Effect of reaction term on the time-concentration curve in problem 1.

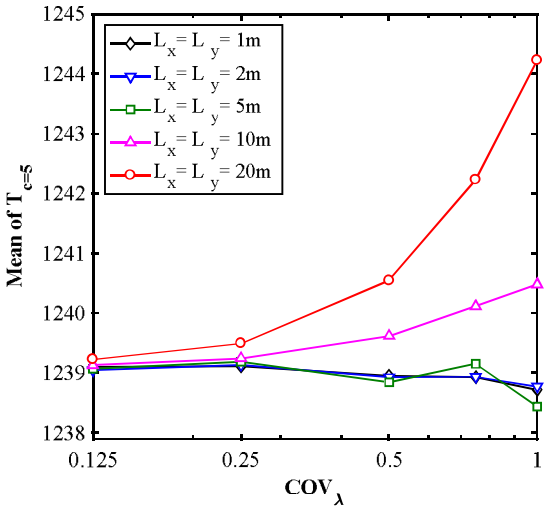

(a)

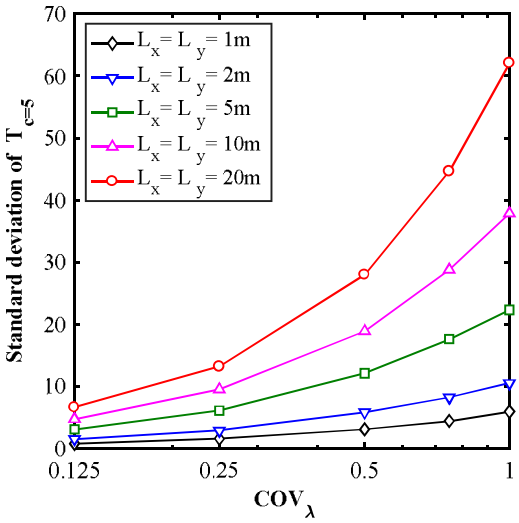

(b)

Fig. 13. Influence of COV and autocorrelation distance for the reaction term on the mass travel time in problem 1. (a) mean of $T_{c=5}$, (b) standard deviation of $T_{c=5}$.

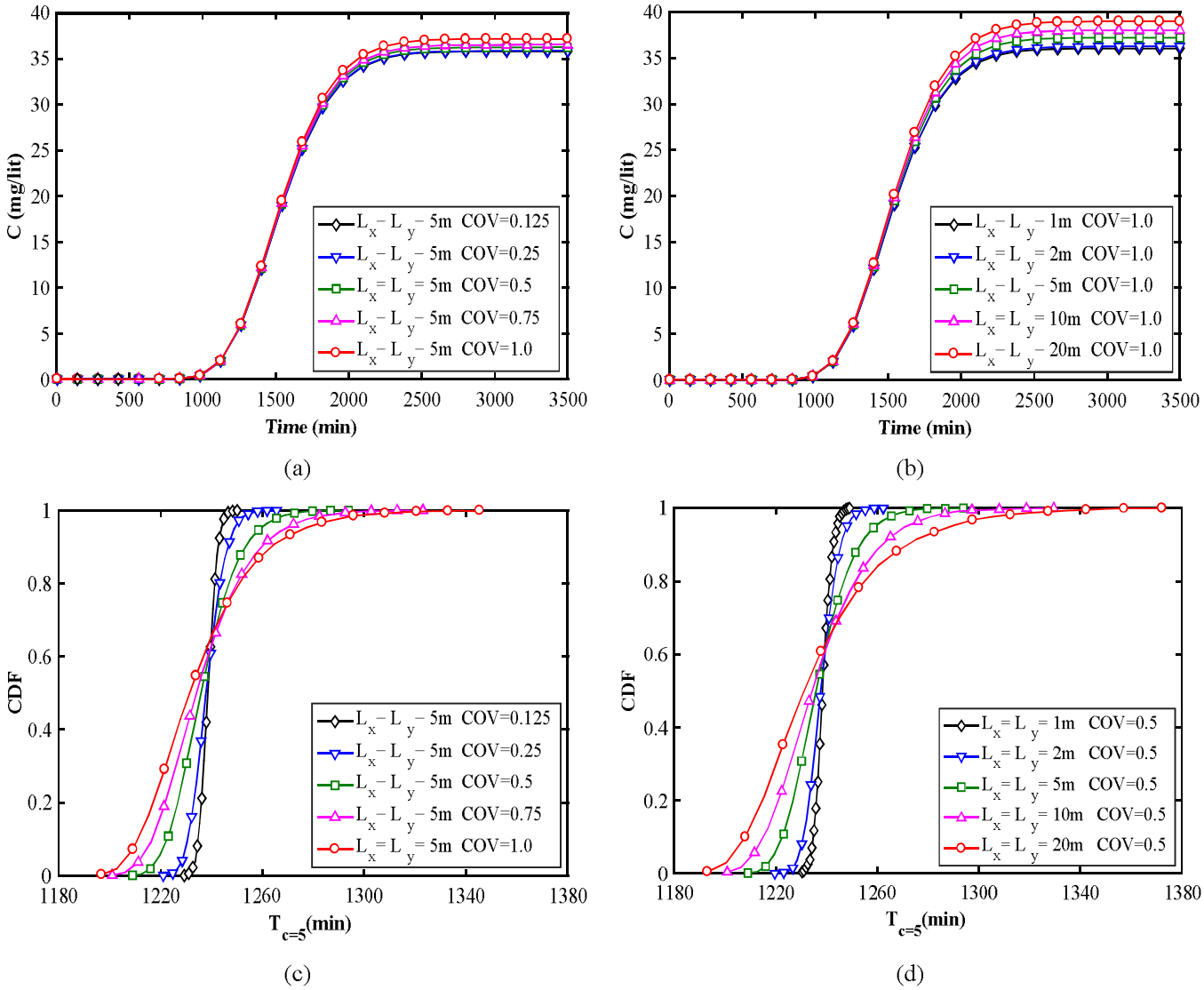

Fig. 14. Influence of stochastic reaction term on the CDF and mean time-concentration curves in problem 1. (a) time-concentration curves resulted from different COV values, (b) time-concentration curves resulted from different autocorrelation distances, (c) CDF curves of $T_{c=5}$ obtained from different COV values, (d) CDF curves of $T_{c=5}$ obtained from different autocorrelation distances.

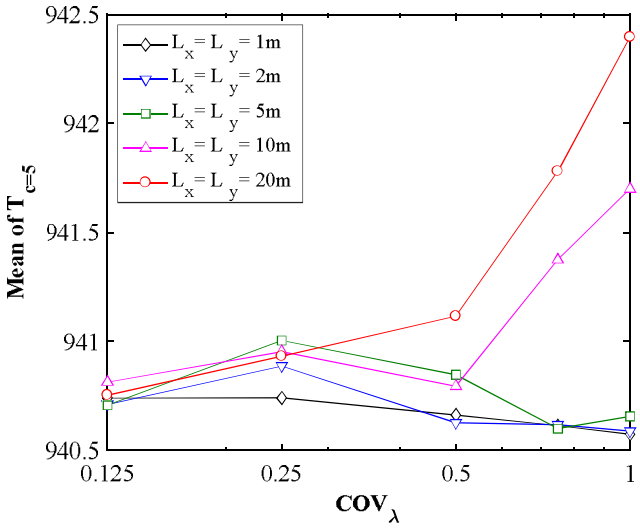

(a)

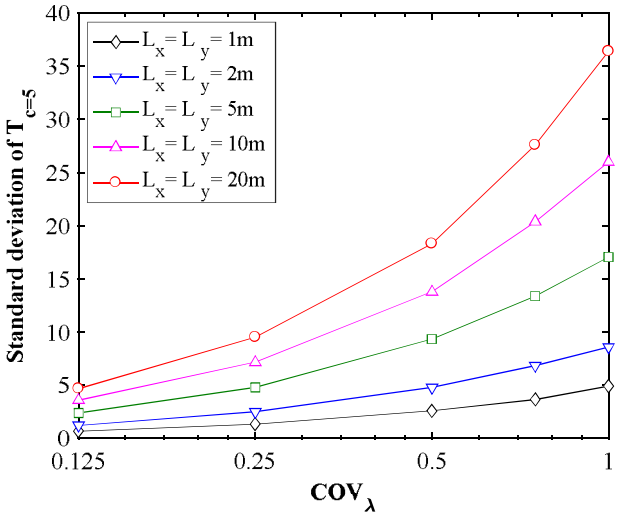

(b)

Fig. 15. Influence of COV and autocorrelation distance for the reaction term on the mass travel time in problem 2. (a) mean of $T_{c=5}$, (b) standard deviation of $T_{c=5}$.

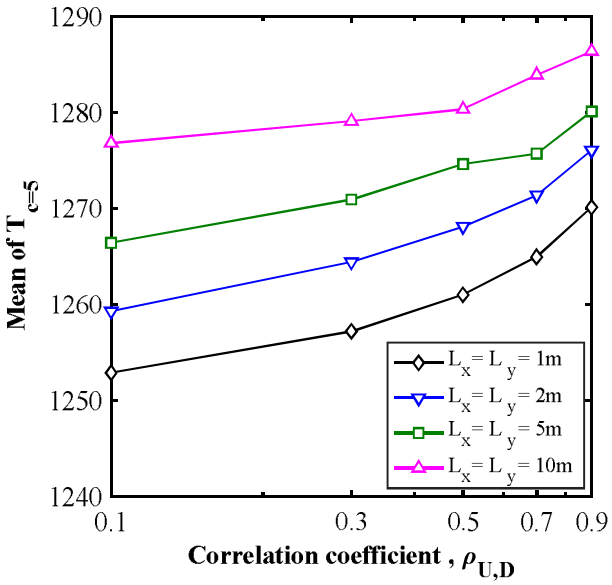

(a)

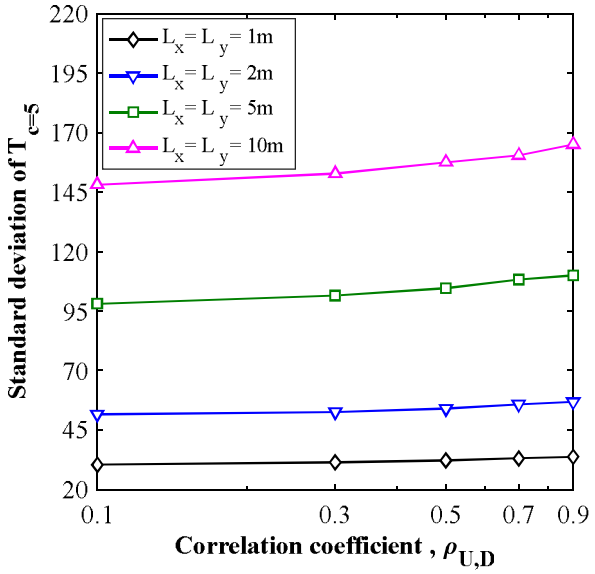

(b)

Fig. 16. Effect of cross-correlation between dispersion coefficient and pore velocity on $T_{c=5}$ in problem 1. (a) mean of $T_{c=5}$ vs. cross-correlation coefficient, (b) standard deviation of $T_{c=5}$ vs. cross-correlation coefficient.

Table 1
Statistical distribution constants of advection-reaction-dispersion equation for the probabilistic simulations.

Parameters	Mean	Coefficients of variations	Autocorrelation distance (m)	Distribution type
D (m^2/min)	0.03	0.125, 0.25, 0.5, 0.75, 1.0	1, 2, 5, 10, 20	Lognormal
U (m/s)	0.03	0.125, 0.25, 0.5, 0.75, 1.0	1, 2, 5, 10, 20	Lognormal
λ (1/min)	0.0005	0.125, 0.25, 0.5, 0.75, 1.0	1, 2, 5, 10, 20	Lognormal

Table 2
Correlation coefficients for different PDFs of $T_{c=5}$ regarding spatial variability of dispersion coefficient.

Autocorrelation distance	Coefficient of variation COV	Correlation coefficient R^2		
		Normal distribution	Lognormal distribution	Skew normal distribution
1 m	0.5	0.987	0.987	0.987
2 m	0.5	0.994	0.994	0.989
5 m	0.125	0.994	0.994	0.994
5 m	0.25	0.993	0.993	0.989
5 m	0.5	0.994	0.993	0.993
5 m	0.75	0.984	0.989	0.985
5 m	1.0	0.974	0.987	0.987
10 m	0.5	0.980	0.990	0.986
20 m	0.5	0.973	0.988	0.990

Table 3
Correlation coefficients for different PDFs of $T_{c=5}$ regarding spatial variability of pore velocity.

Autocorrelation distance	Coefficient of variation COV	Correlation coefficient R^2		
		Normal distribution	Lognormal distribution	Skew normal distribution
1 m	0.5	0.984	0.996	0.993
2 m	0.5	0.979	0.997	0.990
5 m	0.125	0.990	0.994	0.984
5 m	0.25	0.988	0.996	0.994
5 m	0.5	0.956	0.996	0.983
5 m	0.75	0.917	0.997	0.972
5 m	1.0	0.877	0.996	0.952
10 m	0.5	0.927	0.997	0.977
20 m	0.5	0.883	0.989	0.958

Table 4
Correlation coefficients for different PDFs of $T_{c=5}$ regarding spatial variability of reaction term

Autocorrelation distance	Coefficient of variation COV	Correlation coefficient R^2		
		Normal distribution	Lognormal distribution	Skew normal distribution
1 m	0.5	0.973	0.973	0.981
2 m	0.5	0.987	0.987	0.992
5 m	0.125	0.983	0.983	0.985
5 m	0.25	0.991	0.991	0.995
5 m	0.5	0.983	0.984	0.996
5 m	0.75	0.968	0.970	0.997
5 m	1.0	0.957	0.960	0.996
10 m	0.5	0.972	0.974	0.997
20 m	0.5	0.950	0.954	0.996

Table 5
Modified cross-correlation coefficient between U and D for COV=0.25

$\rho_{U,D}$	F	$(\rho_{U,D})_{modified}$
0.1	1.0277	0.1027
0.3	1.0213	0.3064
0.5	1.0151	0.5075
0.7	1.0090	0.7063
0.9	1.0029	0.9027

Conflict of Interest

Dear editor,

There is no conflict of interest in the paper entitled "Probabilistic simulation of advection-reaction-dispersion equation using random lattice Boltzmann method" by Ali Akbar Hekmatzadeh, Ali Adel, Farshad Zarei, and Ali Torabi Haghighi. The authors have no affiliation with any organization with a direct or indirect financial interest in the subject matter discussed in the manuscript. Moreover, this manuscript has not been submitted to, nor is under review at, another journal or other publishing venue.

Sincerely,

Ali Akbar Hekmatzadeh

Assistant Professor, Department of Civil and Environmental Engineering

Shiraz University of Technology